MODELING SPATIAL AND TEMPORAL DISTRIBUTION OF PRECIPITATION IN AN ARIZONA PONDEROSA PINE FOREST ECOSYSTEM

Assefa Desta and Aregai Tecle[1]

Precipitation is governed by physical laws and complex atmospheric processes. Atmospheric processes that generate precipitation systems are complex and spatially and temporally varying, making accurate prediction of precipitation practically difficult. Therefore, precipitation is often evaluated statistically as a random process, in which its future temporal distribution is studied based on its historical distribution pattern (Viessman et al. 2003; Rupp 1995). We developed a stochastic, event-based precipitation model that takes advantage of GIS technology for both cold- and warm-season precipitation events in the ponderosa pine forested watersheds in north-central Arizona. To realistically generate synthetic precipitation data, such a model must consider both the temporal and spatial characteristics of precipitation events in the study area.

The temporal component of the model uses a stochastic process to describe the distribution of precipitation characteristics such as inter-arrival time between events, and the depth and duration of individual storms. The procedure uses appropriate theoretical probability distribution functions and a random number generator to describe and simulate the various precipitation characteristics. The frequency distribution of the inter-arrival time between events is modeled using a univariate Weibull probability distribution function. Depth and duration are modeled using a joint bivariate distribution function to account for their dependency on each other. Using the selected theoretical distribution functions, random numbers are generated for each precipitation characteristic to simulate synthetic time series of precipitation events.

The types of models used depend on the characteristics of the precipitation patterns in the cold and warm seasons in north-central Arizona. Cold-season precipitation events are typically the result of frontal storms coming from the northwest or southwest (Sellers et al. 1985). Storms from the southwest are enhanced by orographic lifting as they rise up the steep side of the Mogollon Rim (Beschta 1976). Warm-season precipitation events are generally monsoonal, convective storms that tend to be highly localized and intensive but short lived, lasting from several minutes to a few hours (Fogel and Duckstein 1969; Fogel et al. 1971). Cold-season precipitation, however, can last more than one day and individual storms may be related to each other by large-scale weather systems. An independent model is used to describe the warm-season precipitation events, whereas cold-season precipitation events are described using a dependent model with additional parameters to adequately describe their characteristics (Duckstein et al. 1975). A test of precipitation models shows that they parallel the cold- and warm-season precipitation patterns in the study area reasonably well; there is reasonable correlation between the simulated and measured relative frequency distributions over the 20 years studied (1962–1982).

We used spatial analysis to define areal distribution of precipitation event depth and duration, as well as the form of precipitation—rain or snow—over the watershed. The event depth and duration at any point on the watershed is described as a function of the point's location in terms of its elevation, aspect, latitude, and longitude, as well as a function of the storm depth and duration simulated at the outlet of the watershed. GIS technology is used with the above functions to generate rasterized images of event depth and duration.

STUDY AREA

We used the largest of the former Beaver Creek experimental watersheds (the Bar M) as a case study to develop the precipitation model. These experimental watersheds are located within the Coconino National Forest in north-central Arizona (Figure 1). The project was established by the Forest Service in 1956 to study the effect of vegetation manipulation on various watershed resources and forest amenities. The outlet of the 6678-hectare Bar

[1]School of Forestry, Northern Arizona University, Flagstaff

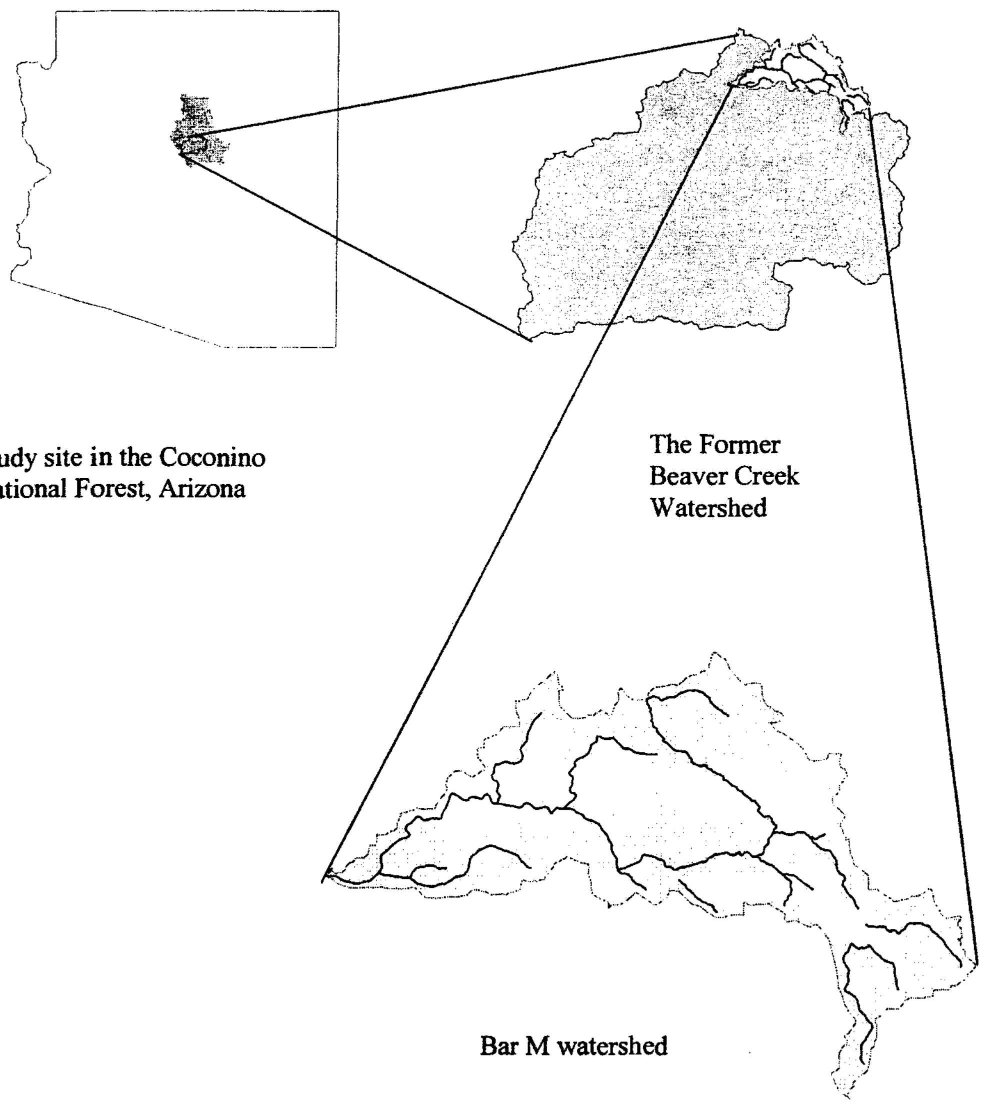

Figure 1. Location of the Bar M watershed in the former Beaver Creek experimental watershed.

M watershed lies at 111° 36' 19" W longitude and 34° 51' 40" N latitude, at 1930 m above sea level; the highest point rises to 2351 m. The watershed is generally inclined southwesterly and has an average slope of 12 degrees. Eighty percent of the Bar M watershed is covered by ponderosa pine (*Pinus ponderosa*), and Gambel oak (*Quercus gambelii*) and aspen (*Populus tremuloides*) cover about 12 and 3 percent of the watershed respectively.

The two major precipitation seasons in the north-central part of Arizona occur in winter and summer. The cold season, which stretches from October 1 to April 30, is mostly characterized by low temperatures and frontal storms (Baker 1982; Rupp 1995). Summer season precipitation events, on the other hand, come mostly in the form of convective precipitation storms during July, August, and September (Baker and Brown 1974).

Winter precipitation in the ponderosa pine type part of the Beaver Creek watershed area averages 431 mm; 60 percent of it comes as snow (Baker 1982). Summer precipitation averages about 216 mm, which is about 33 percent of the annual precipitation (Baker 1982). The highest (18° C) and the lowest (9° C) recorded average monthly summer temperatures occur in July and May, respectively (Campbell and Ryan 1982).

We used precipitation and other climatological data collected between 1962 and 1982 from a network of precipitation gauges in the former Beaver

Creek experimental watersheds. We also used data from the existing multiple-instrumented, state-of-the-art weather and stream gauging facilities at the outlet of the Bar M watershed.

Between 1962 and 1982, approximately 89 precipitation gauges were scattered throughout the area (Figure 2), however all were not operational during the entire 20 years. Some were recording gauges equipped with 24-hour charts, some consisted of standard gauges that were checked weekly, and a few were storage gauges checked at least twice a year. We used only the precipitation data collected from the recording gauges to model the precipitation events.

TEMPORAL ANALYSIS OF PATTERNS

Cold-Season Precipitation

The cold-season precipitation model used in this study follows the one used by Rupp (1995), which is a modified version of the model used by Duckstein et al. (1975). Our model simulates precipitation intensity—the most important variable in determining the amount of surface runoff and water yield.

The first modification to the model involved redefining an "event," which is uninterrupted rainfall or snowfall of any duration, lasting from several minutes to many hours. If it stops raining

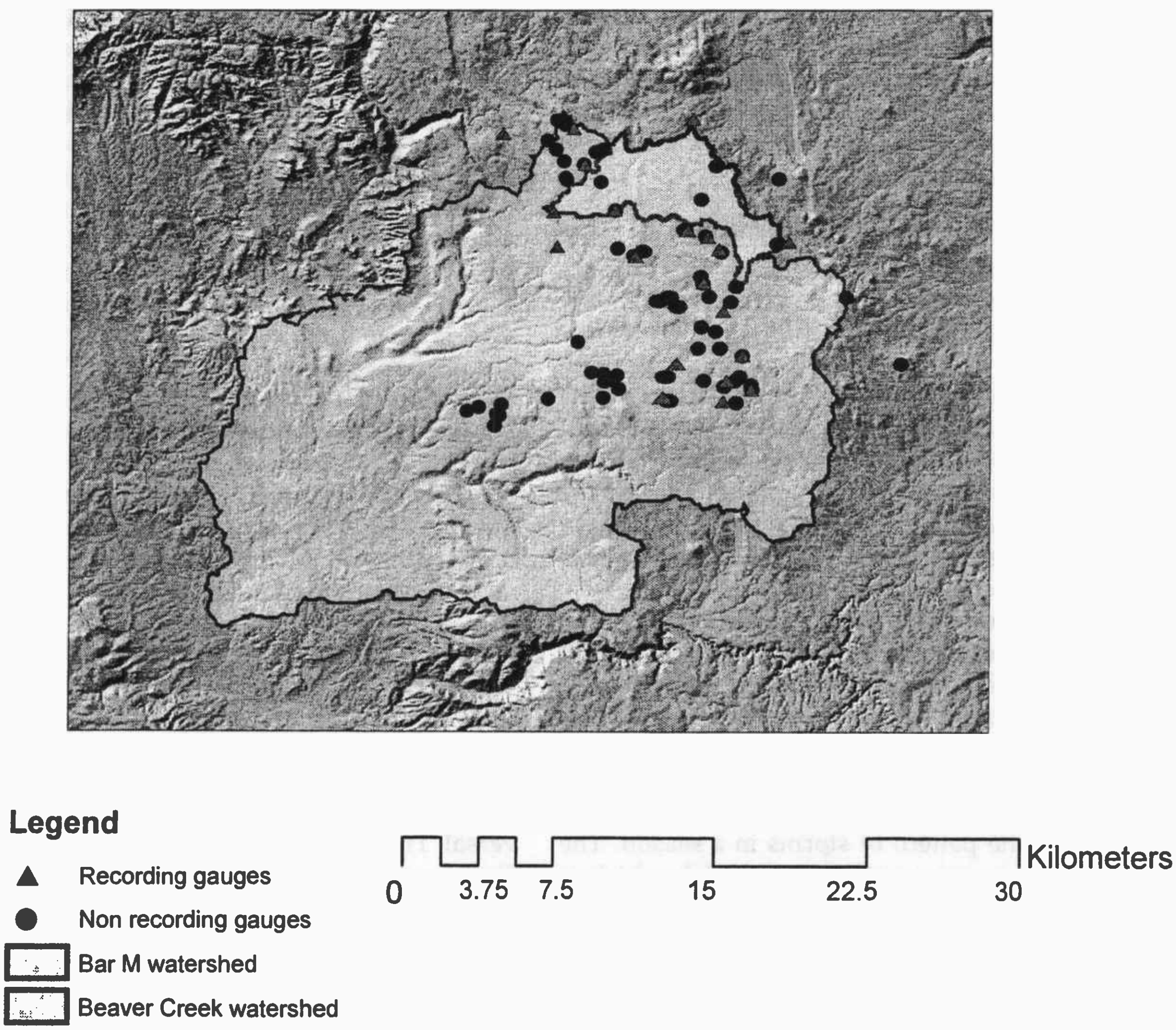

Figure 2. The Bar M watershed and the precipitation gauge network in the former Beaver Creek experimental pilot project.

and then starts again after 5 minutes, the rainfall during the second period is considered a separate event. The second modification was to remove the variable "group." The definition of storm sequence remains the same except for one difference. Duckstein et al. (1975) defined storm sequence as two successive storm events separated by 3 consecutive days of dry weather; their time resolution was 1 day. However, our model recognizes time periods of as little as 5 minutes. For the interval time between storm events, Duckstein et al. (1975) used 2 days for inter-arrival times of 1.5–2.5 days, 3 days for times of 2.5–3.5 days, and so on. For our study the minimum time between consecutive storm sequences was 3.5 days.

The new model, modified from Duckstein et al. (1975) and used in Rupp (1995), is described in terms of the following five variables: time between sequences (days), number of events per sequence, time between events (hrs), precipitation amount per event (mm), and duration of events (hrs). Figures 3 and 4 illustrate the relationships of these variables to each other.

Warm-Season Precipitation

Because consecutive rain events of the convective thunderstorm type are relatively independent from each other, we used an independent event-based model to simulate their temporal distribution (Tecle et al. 1988). We modified the model developed by Bogardi et al. (1988), which dealt with total rainfall depths and durations occurring on consecutive rainy days but did not address the intensity of individual storms. Hence, our modification was needed to allow for the simulation of individual storm event intensities.

The most important change to the model was to redefine an "event," which, as in the cold-season precipitation model, describes uninterrupted rainfall of any duration. The second modification was to remove number of events per season, because our study attempts to describe the general pattern of individual warm-season precipitation events instead of the pattern of storms in a season. The new warm-season precipitation model, which is similar to Bogardi et al. (1988), is described using three variables: precipitation amount per event (mm), duration of events (hrs), and time between events (hrs).

Various theoretical distribution functions have been used in past studies to describe the probability distribution of precipitation characteristics (Eagleson 1972; Duckstein et al. 1973, 1975; Hanes et al. 1977; Rupp 1995). We used SAS statistical software to analyze the observed frequency distribution of the precipitation characteristics while fitting various known theoretical probability distribution functions and identifying the best-fitted model using four goodness-of-fit tests (SAS Institute 2004). Four theoretical probability distribution functions—lognormal, gamma, Weibull, and exponential—were fitted to the frequency distribution of the observed data. Kolmogorov-Smirinov, Cramer–Von Mises, Anderson-Darling, and chi-square tests were used for the goodness-of-fit test to determine appropriate models for the data distributions.

The method of moments is one way of fitting these models to the observed data. The method requires estimating the parameters of the various distribution functions (Barndorff-Nielsen et al. 1996). Some distributions require multiple parameters while others use only one parameter. Parameters of the theoretical distribution functions are estimated from the mean and variance of the observed precipitation characteristics data. Three of the precipitation model variables (time between sequences, number of events per sequence, and time between events) can be described using a univariate probability distribution function (described above). The modeling of depth and duration, however, is more complex because these two variables are not independent of each other. Therefore, a different method was needed, suitable for simulating two dependent random variables. We used a bivariate model, known as ECD, to describe and simulate the dependent variables of depth and duration. The procedure involves explicitly describing the conditional probability distribution of depth, given duration of the event.

SPATIAL ANALYSIS OF EVENTS

We used GIS to describe the spatial distributions of the cold- and warm-season precipitation event characteristics. The various landscape characteristics used for this purpose were gauge elevation, geographic location in terms of Universal Transverse Mercator (UTM), and aspect. Gauge elevation was relevant because many previous studies in the region had already shown that precipitation increases with elevation (Beschta 1976; Campbell and Ryan 1982). Similarly, the UTM coordinates of the gauges were examined to represent the general trend of the Beaver Creek watersheds rising northeastward. Finally, the aspects of the gauge location were analyzed to see if differences in precipitation exist between windward and leeward sites.

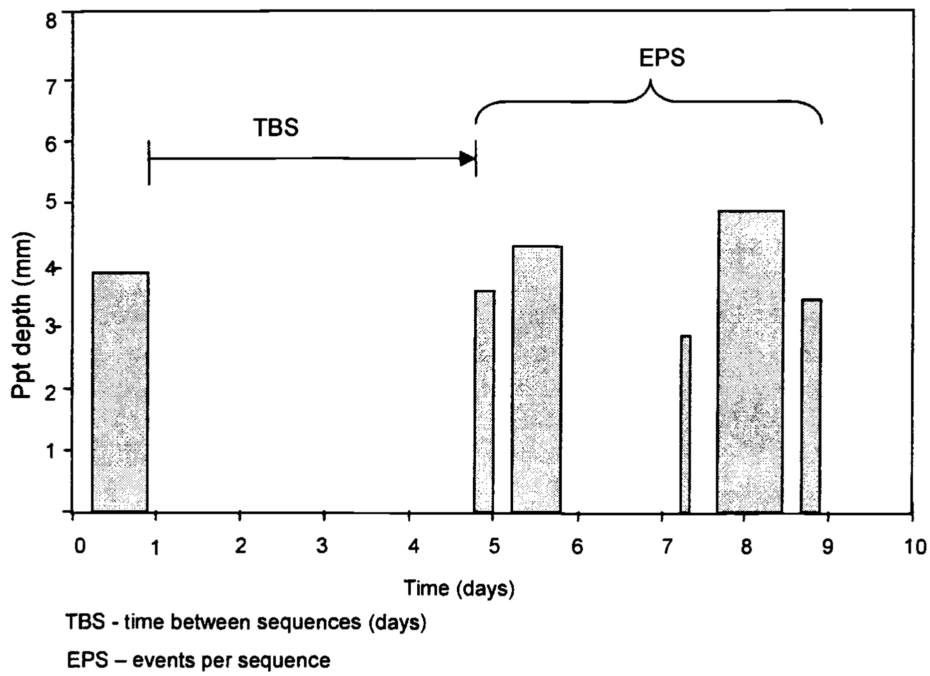

Figure 3. Cold-season model variables for storm sequences.

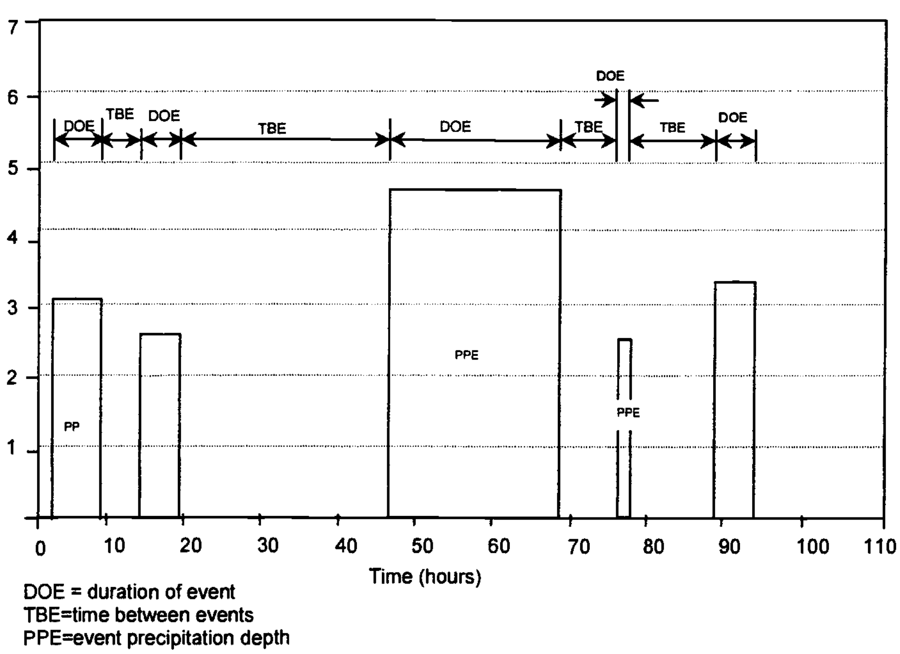

Figure 4. Cold-season and warm-season precipitation model variables for storm events.

The relationships between precipitation depth and the four landscape variables are described in the form of regression equations. After the prediction equations for precipitation depth were determined, we used GIS technology along with the equations to map the spatial distribution of event depth.

Temporal Distribution

Of the four models fitted (lognormal, gamma, Weibull, and exponential) to the time between events data, the Weibull distribution function seems to represent the data better than the others (Figure 5). The distribution of the number of events per sequence was also best described using the Weibull distribution function, whereas gamma distribution seems to fit time between sequences data better. In the case of the joint distributions of depth and duration, the gamma distribution performed best in describing their marginal distribution functions. However, the model failed all the tests at the 5 percent level. We applied the same procedures to each of the precipitation characteristics to determine the best-fit models. The types of models used to describe each variable and the significance levels using the four goodness-of-fit tests are shown in Table 1.

To check the performance of the cold-season precipitation model, we compared the synthetic precipitation data generated by the model with the relative frequency of seasonal total precipitation data actually measured in each cold season during the 20 years of study. The relative frequency histograms of the total measured and simulated data, shown in Figures 6 and 7 respectively, show some differences in the mean and standard deviations of the two data types. The mean and the standard deviation of the seasonal total observed data are 423 and 81.1 mm, whereas those for the simulated data are 482 and 90.2 mm respectively. However, the magnitudes of the most often occurring seasonal total precipitation data for the measured and simulated data are quite similar. The mode of the measured seasonal total is 450 mm, whereas the mode of the simulated seasonal total is 500 mm (see Figures 6 and 7).

We also compared the 20-year seasonal totals of simulated precipitation with those of the observed data to check the performance of the warm-season precipitation model. As shown in the relative frequency histograms of Figures 8 and 9, the differences between the measured and simulated data are small. The mean and standard deviation for the observed seasonal totals are 203 and 58.8

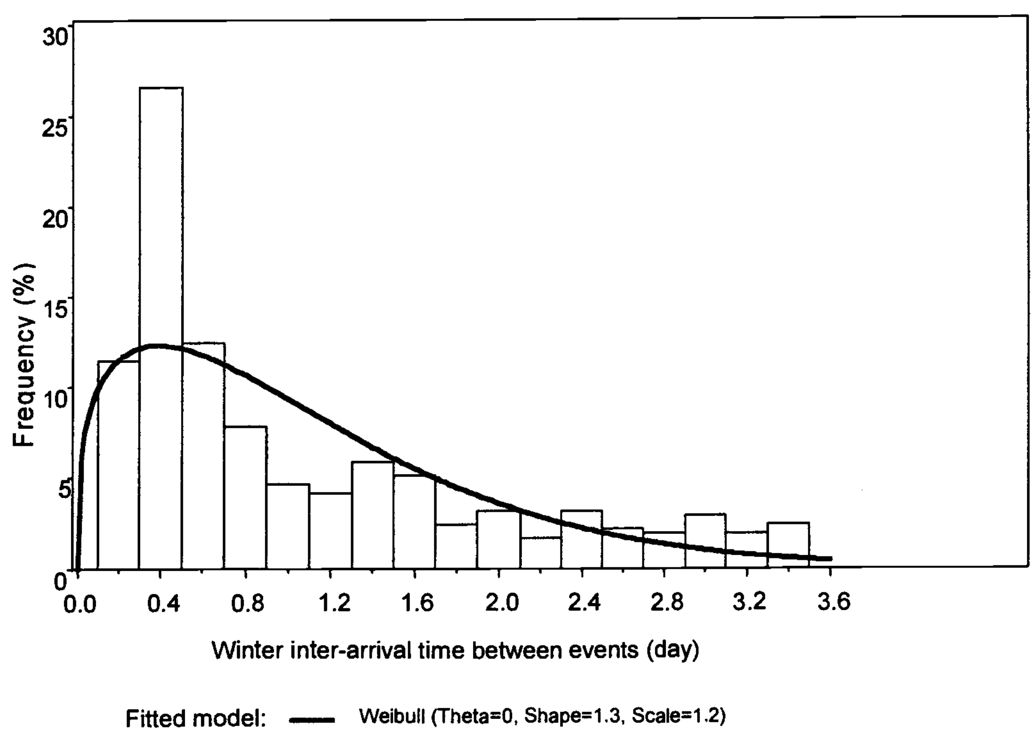

Figure 5. Frequency distribution of inter-arrival time between cold-season events fitted with Weibull probability distribution function (p value = 0.01).

Table 1. The p values for the best-fitted models of cold- and warm-season precipitation events.

Season	Variables	Best-fitted Probability Distribution Functions	Kolmo-gorov-Smirnov	Cramer–Von Mises	Anderson-Darling	Chi-Square	Signi-ficance Level
Cold season	Time between sequence	Gamma	0.5	0.5	0.5	0.184	5%
	No. events per sequence	Weibull	–	0.01	0.01	0.001	5%
	Time between events	Weibull	–	0.01	0.01	0.001	5%
	Duration of events	Gamma	–	–	–	0.035	5%
	Depth of events	Gamma	–	–	–	0.04	5%
Warm season	Time between events	Weibull	–	0.01	0.01	0.001	5%
	Duration of events	Gamma	–	–	–	0.035	5%
	Depth of events	Gamma	–	–	–	0.04	5%

mm, whereas those for the simulated data are 215 and 72.7 mm. The most commonly occurring seasonal precipitation totals in both cases are between 200 and 250 mm. The slight differences between the two data types may be due to data inadequacy and imperfect model fitness. In general, the warm-season precipitation simulation model seems to perform better than the cold-season model.

Spatial Distribution

The spatial variability of the precipitation in the Bar M watershed was analyzed from a subset of the network of precipitation gauges in the Beaver Creek watershed. The selected subset consists of gauges that were operational during the same time period and located nearby to and within the Bar M watershed. Gauges located at elevations much lower than those of the Bar M watershed and in other forest types were excluded. An additional restriction necessary for evaluating storm duration was the use of recording gauges only. Twenty of 89 gauges could fulfill the above criteria for at least a 6-year period. The depths of all the individual storm events were summed separately over the 6-year period to obtain a 6-year total amount of precipitation for each gauge.

A stepwise forward ranking approach was used to select the best predictor from among the four variables and to develop the best-fit regression equation for the change in precipitation depth with space. The best-fit regression equation for the cold-season precipitation depth was expressed in terms of UTM-Y, with little or no contribution from any one of the other three variables (UTM-X, elevation, and aspect; see equation 1). The relationship between UTM-Y and precipitation depth is nonlinear and is expressed using the following third-degree polynomial equation. Based on this equation Figure 10 was constructed to represent the spatial distribution of a particular cold-season precipitation event. As expected, the precipitation event depth increases with an increase in elevation across the entire watershed.

$$P = 2 \times 10^{-13}\,(\text{UTM-Y})^3 - 2 \times 10^{-6}\,(\text{UTM-Y})^2 + 7.827\,(\text{UTM-Y}) - 1 \times 10^7 \quad [1]$$

$$r^2 = 0.748$$

The spatial distribution of precipitation during the warm season is expressed in terms of the multiple variables UTM-X, UTM-Y, and elevation, as shown in equation 2. The r^2 value for this regression equation is 0.45.

$$P = 1.04 \times 10^{-7}\,(\text{UTM-X}) - 4 \times 10^{-6}\,(\text{UTM-Y}) + 3.77 \times 10^{-4}\,(\text{ELEV}) + 16.88 \quad [2]$$

$$r^2 = 0.45$$

Figure 11 represents the spatial distribution of the warm-season precipitation event depth calculated using equation 2. According to the figure, the amount of summer precipitation ranges from 9.6 to 10.8 mm, with the largest amount occurring on the highest elevation parts of the watershed.

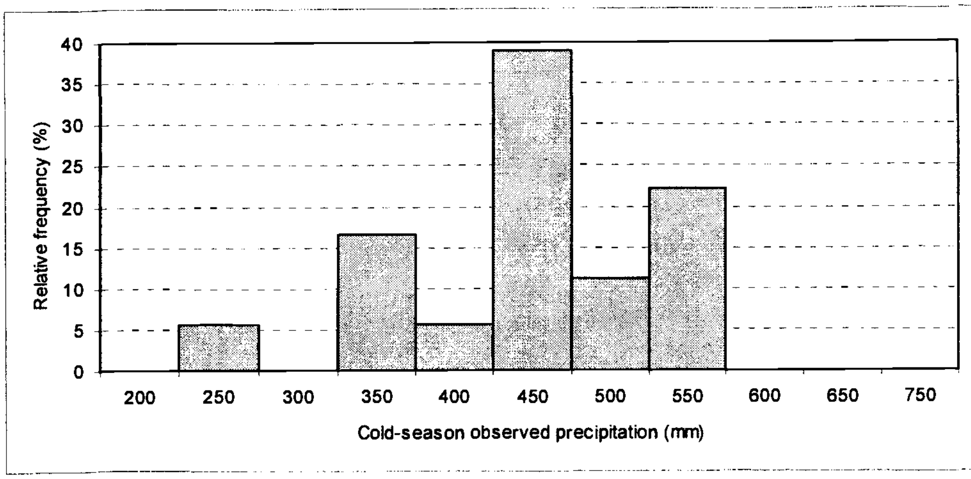

Figure 6. Relative frequency of measured cold-season precipitation total amounts (n = 20 years).

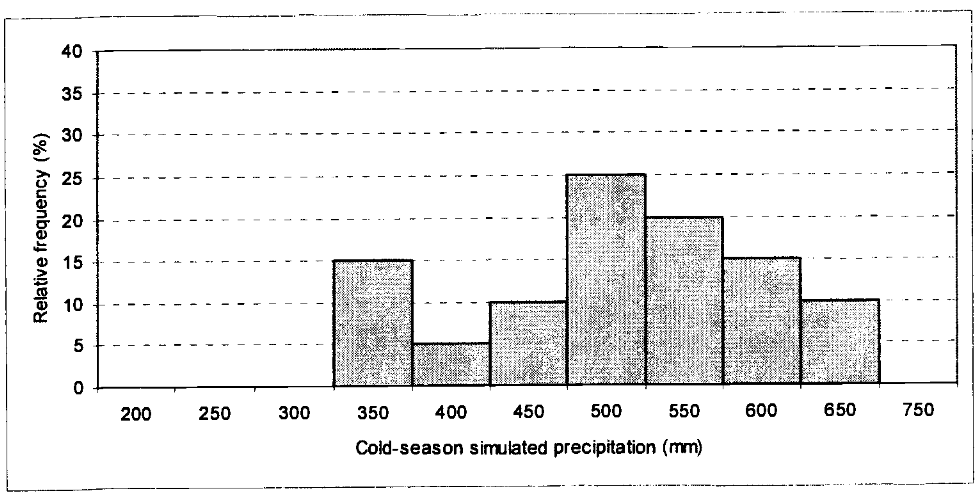

Figure 7. Relative frequency of simulated cold-season precipitation total amounts (n = 20 years).

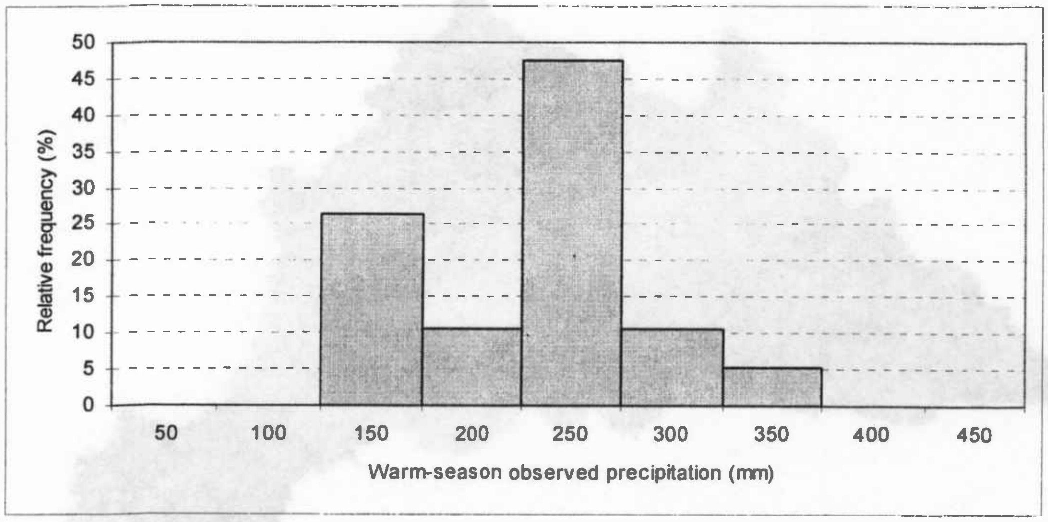

Figure 8. Relative frequency of measured warm-season precipitation total amounts (n = 20 years).

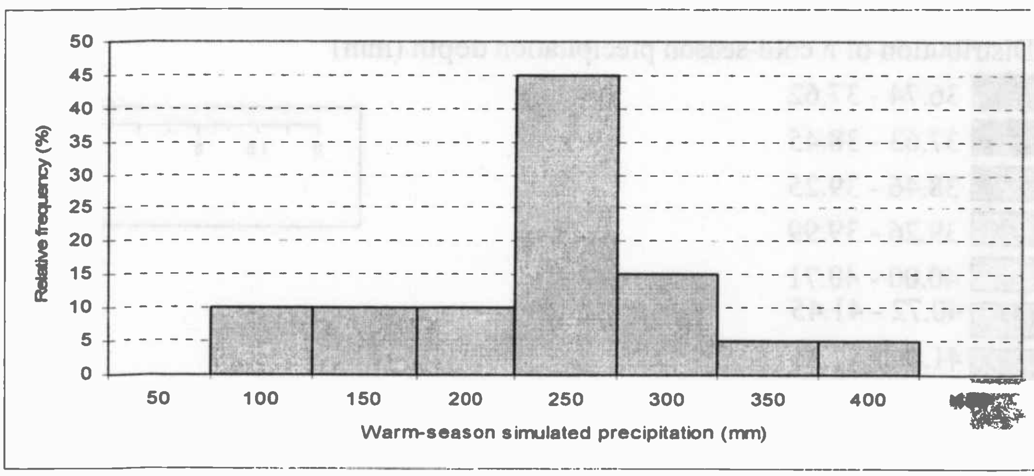

Figure 9. Relative frequency of simulated warm-season precipitation total amounts (n = 20 years).

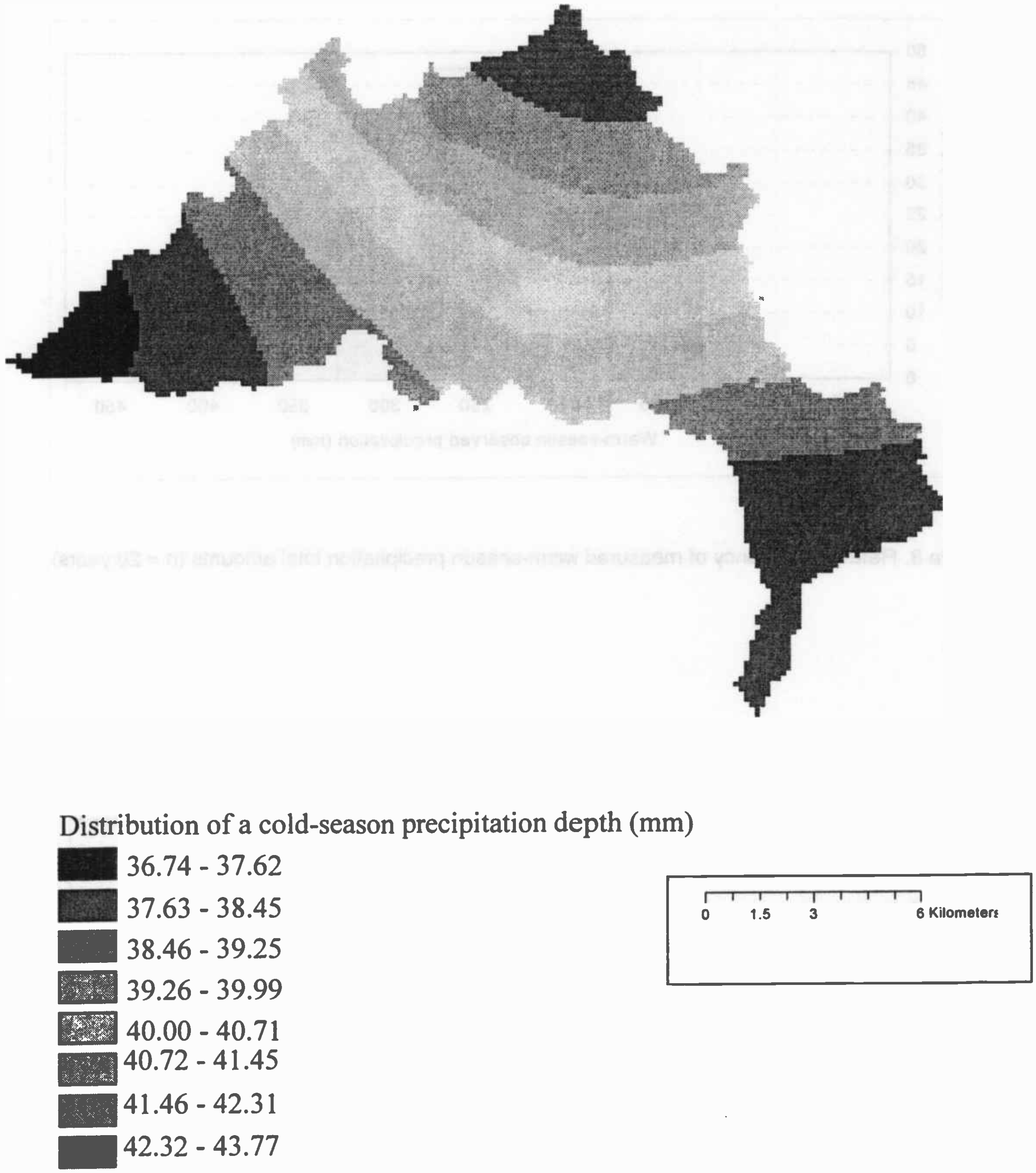

Figure 10. The spatial distribution of a simulated cold-season precipitation event depth.

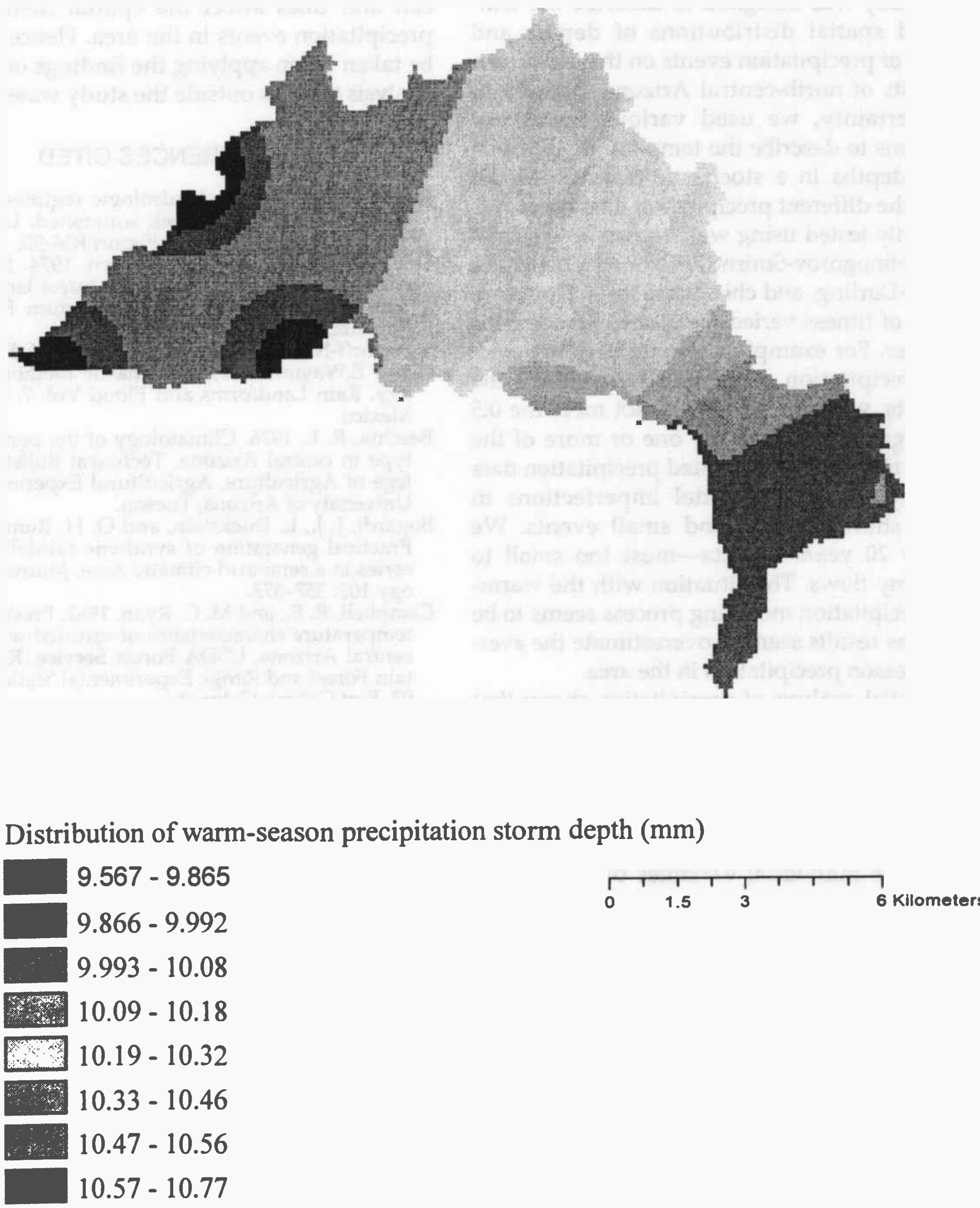

Figure 11. The spatial distribution of a simulated warm-season precipitation storm depth.

SUMMARY AND CONCLUDING REMARKS

This study was designed to describe the temporal and spatial distributions of depths and durations of precipitation events on the ponderosa pine forests of north-central Arizona. Because of data uncertainty, we used various theoretical distributions to describe the temporal distribution of event depths in a stochastic manner. Model fitness to the different precipitation data types was satisfactorily tested using well-known approaches such as Kolmogorov-Smirnov, Cramer–Von Mises, Anderson-Darling, and chi-square tests. However, the levels of fitness varied from one characteristic to the other. For example, the time between cold-season precipitation sequences satisfied all the fitness tests, whereas others did not meet the 0.5 percent significance level for one or more of the tests. This may be due to limited precipitation data availability and some model imperfections in handling short-duration and small events. We used only 20 years of data—most too small to produce any flows. The situation with the warm-season precipitation modeling process seems to be different, as results seem to overestimate the average total season precipitation in the area.

The spatial analysis of precipitation shows that variations in depth and duration of both cold- and warm-season precipitation events are partially explained by the locational characteristics of latitude, longitude, elevation, and aspect of points in the watershed. However, it should be noted that the effects of the individual variables on the spatial distribution of precipitation are different from each other in a season and between seasons. The regression equation for the spatial distribution of cold-season precipitation events is described by latitude (in UTM coordinates) alone, with an r^2 value of 0.65. For the warm season, a multivariate equation consisting of elevation, latitude, and longitude jointly described the spatial distribution of the precipitation depth, with an r^2 value of 0.45. The small r^2 values in both the cold- and warm-season precipitation amounts indicate that significant portions of the spatial variabilities of precipitation depth and duration are left unexplained. Perhaps analysis of individual storms may provide better information on the spatial distribution of precipitation events across the watershed.

There are many factors that may influence the spatial variability of precipitation event depth and duration. For example, the factors controlling the areal distribution of precipitation on watersheds along the Mogollon Rim may be different from those on the Bar M watershed, because the Mogollon Rim is a dominant landscape feature that can and does affect the spatial distribution of precipitation events in the area. Hence, care must be taken when applying the findings of the spatial analysis to areas outside the study watershed.

REFERENCES CITED

Baker, M. B., Jr. 1982. Hydrologic regimes of forested areas in the Beaver Creek watershed. USDA Forest Service General Technical Report RM-90.

Baker, M. B., Jr., and H. E. Brown. 1974. Multiple use evaluations on ponderosa pine forest land. 18th Annual Arizona Watershed Symposium Proceedings, Phoenix, Arizona, September 25.

Barndorff-Nielsen, O. E., V. K. Gupta, V. Perez-Abreu, and E.Waymire. 1996. Stochastic method in hydrology. Rain Landforms and Flood Vol. 7. Guanajuato, Mexico.

Beschta, R. L. 1976. Climatology of the ponderosa pine type in central Arizona. Technical Bulletin 228, College of Agriculture, Agricultural Experiment Station, University of Arizona, Tucson.

Bogardi, J. J., L. Duckstein, and O. H. Rumambo. 1988. Practical generation of synthetic rainfall event time series in a semi-arid climatic zone. Journal of Hydrology 103: 357–373.

Campbell, R. E., and M. G. Ryan. 1982. Precipitation and temperature characteristics of forested watersheds in central Arizona. USDA Forest Service, Rocky Mountain Forest and Range Experimental Station GTR RM-93. Fort Collins, Colorado.

Duckstein, L., M. M. Fogel, and J. L. Thames. 1973. Elevation effects on rainfall: A stochastic model. Journal of Hydrology 18: 21–35.

Duckstein, L., M. M. Fogel, and D. R. Davis. 1975. Mountainous winter precipitation: A stochastic event-based approach. In Proceedings of the National Symposium on Precipitation Analysis for Hydrologic Modeling, pp. 172–188. America Geophysical Union.

Eagleson, P. S. 1972. Dynamics of flood frequency. Water Resources Research (8) 4.

Fogel, M. M, and L. Duckstein. 1969. Point rainfall frequency in convective storms. Water Resources Research (5) 6: 1229–1237.

Fogel, M. M., L. Duckstein, and C. C. Kisiel. 1971. Space-time validation of a thunderstorm rainfall model. Water Resources Bulletin (7) 2: 309–315.

Hanes, W. T., M. M. Fogel, and L. Duckstein. 1977. Forecasting snowmelt runoff probabilistic model. Journal of Irrigation and Drainage Division 103 (IR3): 345–355.

Rupp, D. E. 1995. Stochastic, event-based modeling of upland watershed precipitation-runoff relationships. Master's thesis, Northern Arizona Univ., Flagstaff.

SAS Statistical Software. 2004. SAS Institute, Inc. Cary, North Carolina.

Sellers, W. D., R. H. Hill, and M. R. Sanderson. 1985. Arizona Climate: The Hundred Years. University of Arizona Press, Tucson.

Tecle, A., M. N. Fogel, J. Long, and K. H. Kim. 1988. A reference manual for steps simulating the spatial and temporal distribution of storm rainfall in the Santa Cruz river basin. Report submitted to the Pima County Department of Transportation and Flood Control. School of Renewable Nat. Resources, U of A, Tucson.

Viessman, J. W., G. L. Lewis, and J. W. Knapp. 2003. Introduction to Hydrology. 3rd ed. Harper and Row, New York .